Inhibition of Neutrophil Cathepsin G by Oxidized Mucus Proteinase Inhibitor. Effect of Heparin†

Christian Boudier, Martine Cadène, and Joseph G. Bieth*

Laboratoire d'Enzymologie, INSERM U 392, Université Louis Pasteur de Strasbourg, France

Received December 3, 1998; Revised Manuscript Received March 30, 1999

ABSTRACT: Oxidation of mucus proteinase inhibitor (MPI) transforms Met_{73}, the P_1' residue of its active center into methionine sulfoxide and lowers its affinity for neutrophil elastase [Boudier, C., and Bieth, J. G. (1994) *Biochem. J. 303*, 61−68]. Here, we show that the oxidized inhibitor has also a decreased affinity for neutrophil cathepsin G and pancreatic chymotrypsin. The K_i of the oxidized MPI−cathepsin G complex (1.2 μM) is probably too high to be compatible with significant inhibition of cathepsin G in inflammatory lung secretions. Stopped-flow kinetics shows that, within the inhibitor concentration range used, the mechanism of inhibition of cathepsin G and chymotrypsin by oxidized MPI is consistent with a one-step reaction, $E + I \underset{k_{diss}}{\overset{k_{ass}}{\rightleftharpoons}} EI$, whereas the inhibition of elastase takes place in two steps, $E + I \overset{K_i^*}{\rightleftharpoons} EI^* \underset{k_{-2}}{\overset{k_2}{\rightleftharpoons}} EI$. Heparin, which accelerates the inhibition of the three proteinases by native MPI, also favors their interaction with oxidized MPI. Flow calorimetry shows that heparin binds oxidized MPI with K_d, $\Delta H°$, and $\Delta S°$ values close to those reported for native MPI. In the presence of heparin, oxidized MPI inhibits cathepsin G via a two-step reaction characterized by $K_i^* = 0.22$ μM, $k_2 = 0.1$ s^{-1}, $k_{-2} = 0.023$ s^{-1}, and $K_i = 42$ nM. Under these conditions, in vivo inhibition of cathepsin G is again possible. Heparin also improves the inhibition of chymotrypsin and elastase by oxidized MPI by increasing their k_{ass} or $k_2/K_i^*$and decreasing their K_i. Our data suggest that oxidation of MPI during chronic bronchitis may lead to cathepsin G-mediated lung tissue degradation and that heparin may be a useful adjuvant of MPI-based therapy of acute lung inflammation in cystic fibrosis.–

Oxidation of proteins may have physiological and pathological implications. For instance, oxidatively modified proteins are rapidly degraded by intracellular proteinases, indicating that oxidants may regulate the turnover of proteins (*1*). Oxidants are also able to impair the functional activity of numerous proteins, including proteinase inhibitors such as α_2-macroglobulin (*2*), inter-α-inhibitor (*3*), ovoinhibitor (*4*), plasminogen activator inhibitor 1 (*5*), α_1-proteinase inhibitor (*6*), and mucus proteinase inhibitor (MPI)[1] (*7*). The inactivation of the two latter inhibitors by the H_2O_2/myeloperoxidase system secreted by triggered neutrophils is believed to be an important pathogenic factor in destructive lung diseases such as the adult respiratory distress syndrome, lung emphysema, and cystic fibrosis (*8*−*10*). Theses diseases are characterized by a massive recruitment and activation of neutrophils which release elastase and cathepsin G. These proteinases are thought to cleave lung matrix proteins in an almost unimpaired way if the above antiproteinases are oxidized (*8*, *11*).

MPI is a 11.7 kDa protein produced by secretory cells and found in large amounts in bronchial and cervical mucus (*12*, *13*), seminal plasma (*14*), and salivary gland secretions (*15*). It also occurs in low levels in plasma (*13*), cartilage (*16*), and the lower respiratory tract where it has been shown to be located near elastin fibers (*17*). MPI is composed of a single polypeptide chain of 107 amino acid residues stabilized by eight disulfide bonds. Residues 1−54 and 55−107 show a high degree of identity, suggesting that the inhibitor has evolved by duplication of a single ancestral gene (*18*, *19*). X-ray crystallographic analysis of the MPI-chymotrypsin complex confirms this two-domain organization and indicates that the disulfides form intradomain bridges only (*20*). The two domains are encoded on separate exons (*21*). MPI has 15 lysine and 5 arginine residues, some of which participate in the binding of the inhibitor with heparin (*22*).

MPI is a reversible inhibitor of neutrophil elastase and cathepsin G, and pancreatic chymotrypsin and trypsin (*13*, *14*, *19*, *23*). The chymotrypsin inhibitory loop encompasses residues 67−74 of the C-terminal domain, the P_1-P_1' residues being Leu_{72}-Met_{73} (*20*). Site-directed mutagenesis confirms the involvement of Leu_{72} in the binding of chymotrypsin and suggests that elastase also binds at the same site (*24*). In a previous paper, we have shown that mild oxidation of MPI with N-chlorosuccinimide oxidizes one of the four methionine residues of the inhibitor, namely Met-73, the inhibitor's P_1' amino acid. The oxidized inhibitor still inhibited neutrophil elastase but with a 20-fold lower rate and a 120-fold lower

† We thank AFLM (Association Française pour la Lutte contre la Mucoviscidose) for financial support.

* To whom correspondence should be addressed: INSERM U 392, Faculté de Pharmacie, 74 route du Rhin, F-67400 Illkirch, France. Phone: 33 3 88 67 69 34. Fax: 33 3 88 67 92 42. E-mail: jgbieth@pharma.u-strasbg.fr.

[1] Abbreviations: MPI, mucus proteinase inhibitor (same as the secretory leukoprotease inhibitor, SLPI); MeOSuc, methoxysuccinyl; pNA, *p*-nitroanilide; SBzl, thiobenzylester.

10.1021/bi9828526 CCC: $18.00
Published on Web 06/09/1999

affinity as compared with the native inhibitor (*25*). *N*-Chlorotaurine oxidizes the four methionine residues of MPI but yields a derivative whose kinetic constants for the inhibition of neutrophil elastase are close to those observed with the *N*-chlorosuccinimide-derivatized inhibitor (*26*).

Despite its oxidation, MPI may still be a potent elastase inhibitor in upper airways secretions since its concentration (5 μM, refs *27* and *28*) is much larger than its K_i (10 nM, ref *25*). We wanted to see whether the same is true for cathepsin G whose activity is also inhibited by MPI (*19*, *29*). This serine proteinase occurs in the azurophil granules of human neutrophils in amounts equivalent to those of elastase (*30*). It is a cationic glycoprotein whose tertiary structure has been solved recently (*31*). Like elastase, cathepsin G is able to cleave lung connective tissue proteins such as elastin, collagen, proteoglycans, and fibronectin (*11*). In addition, it potentiates the elastolytic activity of neutrophil elastase (*32*). It therefore participates in lung connective tissue degradation during chronic bronchitis and cystic fibrosis. Its inhibition by oxidized MPI has never been studied.

Heparin has been shown to accelerate the inhibition of cathepsin G and elastase by native MPI (*33*−*35*). This anionic glycosaminoglycan mostly consists of trisulfated disaccharide units formed of L-iduronic acid-2-sulfate linked to D-glucosamine-*N*-3,6-sulfate. These regular sequences are variously interrupted by irregular sequences containing either undersulfated or oversulfated uronic or glucuronic acid and amino-sugar residues (*36*). Heparin forms a tight complex with and alters the conformation of native MPI (*33*, *34*). It is not known whether it also interacts with oxidized MPI and activates the inhibitor.

The present paper describes a stopped-flow kinetic investigation of the inhibition of cathepsin G by native and oxidized MPI in the absence and presence of heparin. Since cathepsin G has a chymotrypsin-like specificity and the effect of heparin on the inhibition of elastase by oxidized MPI has not been investigated previously (*25*), we have also done a detailed kinetic study of the effect of oxidation and heparin on the inhibition of chymotrypsin and elastase by MPI.

EXPERIMENTAL PROCEDURES

The source and active-site titration of human leukocyte elastase and cathepsin G, bovine pancreatic chymotrypsin, and human recombinant MPI were the same as described previously (*37*). Oxidized MPI was prepared by reacting the native inhibitor with *N*-chlorosuccinimide under conditions that fully and selectively convert the surface-exposed P'_1 methionine 73 into methionine sulfoxide. Active-site titration of oxidized MPI was done using active-site titrated leukocyte elastase (*25*). All enzyme and inhibitor concentrations cited in this article are referred to as active molecule concentrations. MeOSuc-$(Ala)_2$-Pro-Val-pNA, Suc-$(Ala)_2$-Pro-Phe-pNA and Suc-$(Ala)_2$-Pro-Phe-SBzl were from Bachem (Bubendorf, Switzerland). MeOSuc-$(Ala)_2$-Pro-Ala-SBzl was purchased from ESP (Livermore, CA). Stock solutions of substrates and dithiodipyridine (Sigma) were made in dimethylformamide whose final concentration in the reaction mixtures was 2% (v/v). Heparin was a 4.5 ± 0.5 kDa fragment with low polydispersity whose preparation has been described previously (*34*). All experiments were done at 25 °C in 50 mM Hepes and 100 mM NaCl, pH 7.4, a solution that will be referred to as "the buffer" throughout.

Microcalorimetric Study of the Oxidized MPI:Heparin Binding. The equilibrium dissociation constant K_d, the binding stoichiometry, and the thermodynamic parameters of the complex between oxidized MPI and 4.5 kDa heparin were determined by isothermal microcalorimetric titration at 25 °C using a heat conduction microcalorimeter (2277 Thermal Activity Monitor, ThermoMetric AB, Järfälla, Sweden) equipped with a flow-mix device as previously described (*34*, *38*). The binding curves were obtained by injecting at the same flow rate (3.5×10^{-3} mL s^{-1}) the buffered solutions of oxidized MPI (final concentration, 2 μM) and of heparin (final concentration, 0.8−8 μM) into the flow-mix cell. The thermal power, i.e., the rate of heat production, generated by the formation of the complex was continuously monitored until it reached an equilibrium value (10−15 min).

Enzymatic Methods. The rate of substrate cleavage was monitored by recording the absorbance at 410 or 324 nm for the para-nitroanilides or the thiobenzylesters, respectively. When the later substrates were used, 3 mM dithiodipyridine was included in the reaction medium to trapp the released benzylthiol. The Michaelis constants K_m for the substrate hydrolyses were determined by classical means in the absence or presence of a saturating concentration of heparin (40 μM).

Most kinetic constants were determined using the progress curve method which consists of rapidly mixing enzyme + inhibitor + substrate and recording the release of product (*29*, *39*). At time zero, 1 vol of a buffered solution of enzyme ± heparin was added to 1 vol of a buffered solution of inhibitor + substrate in an observation cell. Substrate hydrolysis was continuously followed for at least 50 s using an Uvikon 941 computerized spectrophotometer (Kontron) equipped with a SFA-11 fast mixing accessory (High-Tech Scientific, Salisbury, U.K.). Data analysis was done using the Enzfitter software (Biosoft, Cambridge, U.K.). When faster reactions were followed, mixing of the reagents and data acquisition were performed with a PQ/SF-53 stopped-flow apparatus (High-Tech Scientific) connected to a HP 3000 microcomputer loaded with the High-Tech HS 1.1 data acquisition and nonlinear regression analysis software. Four hundred time/absorbance pairs were generated per stopped-flow run. All experiments were done under pseudo-first-order conditions, i.e., $[I]_o \geq 10[E]_o$, the enzyme concentration, and the nature of the substrate, and its concentration being chosen such as to yield both detectable progress curves and minimal substrate consumption. The experimental details are given in the Results and Discussion.

Enzyme and inhibitor being reacted under pseudo-first-order conditions and substrate being not depleted to a significant extent during the runs, the progress curves may be described using the following equation (*39*):

$$[P] = v_s t + \frac{v_z - v_s}{k}(1 - e^{-kt}) \qquad (1)$$

where [P] is the product concentration at any time t, v_z is the velocity at $t = 0$, and v_s is the steady-state velocity. The progress curves were fitted to eq 1 by nonlinear least-squares analysis to obtain the best estimates of v_z, v_s, and k. The variation of k as a function of inhibitor concentration was analyzed assuming either that the inhibition conforms to a

Table 1: Kinetic Parameters Describing the Inhibition of Cathepsin G, Chymotrypsin and Elastase by Native and Oxidized MPI in the Absence and Presence of Heparin at pH 7.4 and 25 °C[i]

				kinetic parameters			
						K_i (M)	
proteinase	inhibitor	heparin	inhibition mechanism	k_{ass} or k_2/K_i^* (M^{-1} s^{-1})	k_{diss} or k_{-2} (s^{-1})	calcd	exptl
cathepsin G	native MPI	-	one-step	1.0×10^5	3.5×10^{-3}	3.5×10^{-8}	2.1×10^{-8}
cathepsin G	native MPI	+	one-step	4.0×10^6 [a]	nd	nd	nd
cathepsin G	oxidized MPI	-	one-step	nd	nd	nd	1.2×10^{-6}
cathepsin G	oxidized MPI	+	two-step	4.7×10^5 [b]	2.3×10^{-2}	4.2×10^{-8}	2.4×10^{-8}
chymotrypsin	native MPI	-	one-step	6.5×10^5 [a]	2.6×10^{-5} [c]		4.0×10^{-11} [d]
chymotrypsin	native MPI	+	one-step	6.4×10^6 [a]	nd	nd	nd
chymotrypsin	oxidized MPI	-	one-step	8.8×10^4	7.6×10^{-3}	8.6×10^{-8}	2.0×10^{-8}
chymotrypsin	oxidized MPI	+	one-step	2.8×10^6	1.7×10^{-2}	6.1×10^{-9}	2.6×10^{-9}
elastase	native MPI	-	one-step	3.1×10^6 [e]	1.0×10^{-4} [c]	4.4×10^{-9}	3.3×10^{-11} [e]
elastase	native MPI	+	two-step	2.6×10^7 [e,f]	1.0×10^{-3} [c]	1.4×10^{-9}	3.7×10^{-11} [e]
elastase	oxidized MPI	-	two-step	5.6×10^5 [g]	2.7×10^{-3}		1.0×10^{-8}
elastase	oxidized MPI	+	two-step	1.7×10^7 [h]	2.4×10^{-2}		2.7×10^{-9}

[a] From ref *35*. [b] $k_2 = 0.1$ s^{-1}, $K_i^* = 2.2 \times 10^{-7}$ M. [c] Calcd from K_i and k_{ass} or k_2/K_i^*. [d] From ref *37*. [e] From ref *34*. [f] $k_2 = 2.2$ s^{-1}, $K_i^* = 8.6 \times 10^{-8}$ M. [g] $k_2 = 3.3 \times 10^{-2}$ s^{-1}, $K_i^* = 5.8 \times 10^{-8}$ M. [h] $k_2 = 0.73$ s^{-1}, $K_i^* = 4.1 \times 10^{-8}$ M. [i] The relative errors on the experimental values of k_{ass}, k_{diss}, k_2, k_{-2}, K_i, and K_i^* are ≤30% while those on the calculated parameters k_2/K_i^* and K_i are ≤60%. K_i was calculated from k_{diss} and k_{ass} (one-step inhibition) or from k_2, k_{-2}, and K_i^* (two-step inhibition). nd = not done.

simple bimolecular reaction as shown in Scheme 1

Scheme 1

$$E + I \underset{k_{diss}}{\overset{k_{ass}}{\rightleftharpoons}} EI$$

or that the enzyme and the inhibitor react via a two-step mechanism as shown in Scheme 2

Scheme 2

$$E + I \underset{k_{-1}}{\overset{k_1}{\rightleftharpoons}} EI^* \underset{k_{-2}}{\overset{k_2}{\rightleftharpoons}} EI$$

where E stands for free or heparin-bound proteinase, I is free or heparin-bound MPI, EI* is a rapidly forming preequilibrium complex whose concentration is governed by $K_i^* = k_{-1}/k_1$, and EI is the final enzyme−inhibitor complex.

Schemes 1 and 2 predict eqs 2 and 3, respectively (*29*, *39*):

$$k = \frac{k_{ass}[I]_o}{1 + [S]_o/K_m} + k_{diss} \quad (2)$$

$$k = \frac{k_2[I]_o}{[I]_o + K_{i(app)}^*} + k_{-2} \quad (3)$$

where $K_{i(app)}^* = K_i^*(1 + [S]_o/K_m)$.

A linear plot of k versus $[I]_o$ will thus yield $k_{ass}/(1 + [S]_o/K_m)$ and k_{diss} while a hyperbolic plot provides k_2, k_{-2}, and $K_{i(app)}^*$. Linear or nonlinear regression analysis yields then the best estimates of the kinetic constants. A two-step inhibition does not necessarily yield a hyperbolic dependence of k versus $[I]_o$: if the largest $[I]_o$ used is significantly lower than $K_{i(app)}^*$, eq 3 becomes $k = k_2[I]_o/K_i^*(1 + [S]_o/K_m) + k_{-2}$, a linear relation that resembles eq 2. Observation of a linear k versus $[I]_o$ dependence does, therefore, not exclude a two-step reaction.

The equilibrium dissociation constant of the final enzyme−inhibitor complex EI was calculated from $K_i = k_{diss}/k_{ass}$ for one-step inhibition or from $K_i = K_i^*(k_{-2}/k_2 + k_{-2})$ for two-step inhibition. K_i was also determined directly from steady-state rates v_s (eq 1) measured at $[I]_o \gg [E]_o$ (ref *39*):

$$v_s = \frac{V_m}{1 + K_m/[S]_o(1 + [I]_o/K_i)} \quad (4)$$

or from relative steady-state rates a measured at $[I]_o \approx [E]_o$ (ref *29*):

$$a = 1 - \frac{([E]_o + [I]_o + K_{i(app)}) - \sqrt{[[E]_o + [I]_o + K_{i(app)}]^2 - 4[E]_o[I]_o}}{2[E]_o} \quad (5)$$

RESULTS AND DISCUSSION

Inhibition of Cathepsin G by Native and Oxidized MPI. Using conventional enzymatic methods, Smith and Johnson (*40*) and Thompson and Ohlsson (*19*) reported K_i values of 4.2 and 5 nM for the complex between native MPI and cathepsin G, respectively. We have reinvestigated the inhibition kinetics using our buffer conditions and the progress curve method with stopped-flow mixing and detection. The progress curves were recorded following addition of cathepsin G to buffered mixtures of MPI and Suc-Ala_2-Pro-Phe-SBzl. The final concentrations of enzyme and substrate were 20 nM and 0.21 mM, respectively. The pseudo-first-order rate constant k varied linearly with the native MPI concentration, indicating that under our experimental conditions no reaction intermediate accumulates to a significant extent (Scheme 1). The rate constants k_{ass} and k_{diss} were calculated from a plot in accordance with eq 2 (not shown) using $K_m = 35$ μM determined from a separate experiment and are reported in Table 1. The calculated K_i (35 ± 17 nM) was close to that measured from steady-state velocities (21 ± 4 nM). The K_i for the native MPI−cathepsin G complex is thus 7−8-fold higher that those reported previously (*19*, *40*). In addition, it is 1000-fold higher than that of the native MPI−elastase complex (*34*). Despite its relatively low affinity for cathepsin G, native MPI may be considered a physiological inhibitor of this enzyme in upper airways secretions since its concentration (5 μM, refs *27* and *28)* is

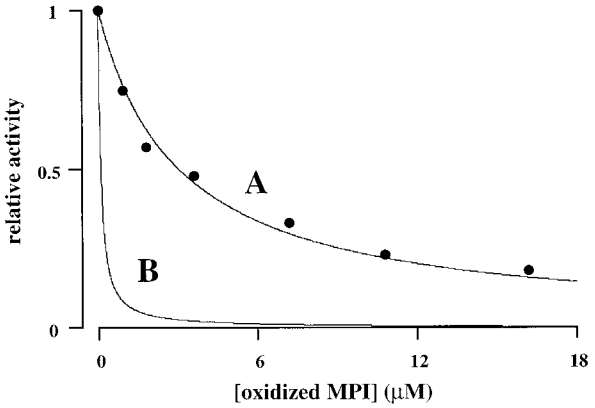

FIGURE 1: Determination of the equilibrium dissociation constant K_i of the cathepsin G:oxidized MPI complex at pH 7.4 and 25 °C. Increasing concentrations of inhibitor were reacted with constant concentrations of cathepsin G (10 nM). After 45 min, a time sufficient to ensure maximal inhibition, 50 μM Suc-Ala$_2$-Pro-Phe-SBzl was added to the mixtures to measure the steady-state velocities: relative activity = velocity in the presence of inhibitor/velocity in its absence. Curve A has been calculated using the best estimate of $K_{i(app)}$ obtained by fitting the data to eq 5 by nonlinear regression analysis. Curve B is a theoretical titration curve describing the inhibition of cathepsin G by oxidized MPI in the presence of 4.5 kDa heparin. This curve has been calculated using 10 nM cathepsin G, and $K_{i(app)} = 0.1$ μM derived from $K_i = 42$ nM (Table 1), and an $[S]_o/K_m$ ratio of 1.4 identical to that used to measure the K_i in the absence of heparin.

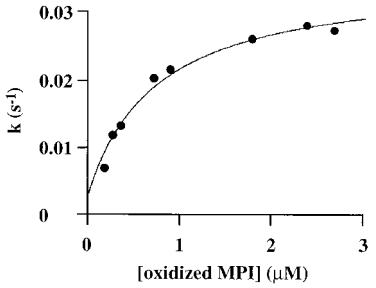

FIGURE 2: Effect of oxidized MPI on *k*, the pseudo-first-order rate constant of elastase inhibition at pH 7.4 and 25 °C. The rate constants *k* were calculated from progress curves recorded following addition of elastase to mixtures of oxidized MPI + MeOSuc-Ala$_2$-Pro-Val-pNA. The final concentrations of elastase and substrate were 20 nM and 1 mM, respectively.

140-fold higher than its K_i. In theory (*29*), under such conditions, it is predicted that >99% of released cathepsin G is inhibited by native MPI at equilibrium.

With the oxidized MPI−cathepsin G system all progress curves were linear, indicating that enzyme, inhibitor, and substrate were in rapid equilibrium and that k_{ass} and k_{diss} could not be determined separately. K_i was therefore measured directly using the equilibrium titration experiment reported in Figure 1 and fitting the data to eq 5 which yielded $K_i = 1.2$ μM (see Table 1), a value 35-fold higher than that found for the interaction between the native inhibitor and cathepsin G. It is likely that during lung inflammation MPI is fully oxidized in the vicinity of triggered neutrophils. Cathepsin G released from these neutrophils will thus be poorly inhibited since the oxidized MPI/K_i ratio will only be equal to 4.2 so that only 80% of enzyme will be inhibited at equilibrium. In addition, its being a low affinity inhibitor renders oxidized MPI very susceptible to substrate competition. This is illustrated in Figure 1, which shows that 5 μM oxidized MPI yields only 62% inhibition of cathepsin G activity in the presence of substrate, although the concentration of the latter is rather low ($[S]_o/K_m = 1.4$). Although we did not use lung extracellular matrix proteins instead of synthetic substrates to evaluated the in vivo inhibitory potency of oxidized MPI, we may suggest that the modified inhibitor poorly protects lung tissues against the deleterious action of cathepsin G.

Inhibition of Chymotrypsin by Oxidized MPI. Neutrophil cathepsin G is a chymotrypsin-like serine proteinase. We therefore studied the effect of MPI oxidation on the inhibition of pancreatic chymotrypsin. Bovine pancreatic chymotrypsin forms a tight complex with native MPI (*24*, *37*) and associates in one step with the inhibitor (*35*). The kinetic parameters describing this enzyme−inhibitor system are reported in Table 1. The kinetics of inhibition of chymotrypsin by oxidized MPI was assessed using progress curves recorded following addition of chymotrypsin to buffered mixtures of oxidized MPI and 0.25 mM Suc-Ala$_2$-Pro-Phe-pNA. The final concentration of chymotrypsin was ≥15 nM. The rate constant *k* was found to increase linearly with the inhibitor concentration (data not shown), indicating that, within the inhibitor concentration range used, the mechanism of inhibition is consistent with a one-step reaction (Scheme 1). Linear regression analysis based on eq 2 and use of $K_m = 42$ μM gave $k_{ass} = 8.8 \times 10^4$ M^{-1} s^{-1} and $k_{diss} = 7.6 \times 10^{-3}$ s^{-1} (Table 1). The calculated K_i (86 ± 39 nM) is statistically different from K_i determined under steady-state conditions (20 ± 5 nM) (Table 1). The two constants are however of the same order of magnitude, and both of them are much higher than the K_i for the native inhibitor (*37*).

Inhibition of Elastase by Oxidized MPI. The kinetics of inhibition of elastase by the oxidized inhibitor was also assessed using the progress curve method. Figure 2 shows that *k* varies hyperbolically with the inhibitor concentration, suggesting that a fast preequilibrium precedes the formation of the final enzyme−inhibitor complex (Scheme 2). Indeed, the data could be fit to eq 3 by nonlinear regression analysis, which yielded the best estimates of $K_{i(app)}^*$, k_2, and k_{-2}, i.e., 0.74 μM, 3.3×10^{-2} s^{-1}, and 2.7×10^{-3} s^{-1}, respectively. The theoretical curve calculated using eq 3 and these estimates fairly well fits the experimental points (see Figure 2). K_i^*(58 nM) was calculated from $K_{i(app)}^*$ using $[S]_o = 1$ mM and $K_m = 0.085$ mM determined in a separate experiment. The calculated K_i (4.4 ± 2.6 nM) was found to agree with that derived from steady-state rate determinations (10 ± 3 nM) (Table 1). On the other hand, the calculated second-order association rate constant $k_2/K_i^* = 5.6 \times 10^5$ M^{-1} s^{-1} and the first-order dissociation rate constant $k_{-2} = 2.7 \times 10^{-3}$ s^{-1} are in good agreement with the association and dissociation rate constants $k_{ass} = 2.6 \times 10^5$ M^{-1} s^{-1} and $k_{diss} = 2.9 \times 10^{-3}$ s^{-1} determined previously using ordinary kinetics and low oxidized inhibitor concentrations, conditions under which EI* is not seen kinetically (*25*).

Despite the use of high inhibitor concentrations and stopped-flow kinetics, the inhibition of elastase by native MPI was found to conform to a simple bimolecular reaction (Scheme 1) which has been assumed to be a two-step reaction (Scheme 2) with $K_i^* > 2$ μM and $k_2 > 6$ s^{-1} (*34*). Thus, transformation of P_1' methionine into methionine sulfoxide favors the formation of EI* (K_i^*decreases by more than 34-fold) but considerably hinders the conversion of EI* into EI

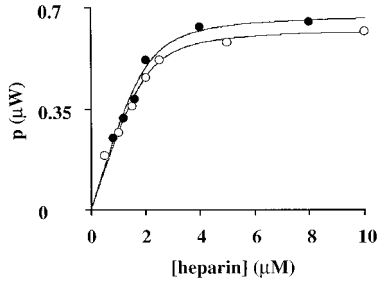

FIGURE 3: Microcalorimetric determination of the equilibrium dissociation constant K_d of the complex formed of oxidized MPI and 4.5 kDa heparin (●) at pH 7.4 and 25 °C. K_d was calculated from the thermal power p using a nonlinear fit of the data to eq 6. The data obtained for native MPI (○) (ref *38*) have been included for the sake of comparison.

(k_2 decreases by more than 180-fold) (see Table 1). The overall effect of oxidation is a 5.5-fold decrease in the association rate constant, a 27-fold increase in the dissociation rate constant, and 133-fold increase in K_i (see Table 1).

If one assumes that, during acute lung infections, oxidation extends to the bulk of MPI (~5 μM, refs *27* and *28*), it follows that the oxidized MPI concentration will be about 1000-fold higher than K_i, indicating that tight-binding inhibition, a prerequisite for in vivo inhibitory function (*41*) does occur despite oxidation of the inhibitor. This reinforces our previously stated view (*25*). To be efficient in vivo, inhibition should not only be tight but also fast enough to prevent undesirable degradation of biological substrates during formation of the inhibitory complex (*29*, *41*). At first sight, elastase is inhibited slower by oxidized MPI ($k_2/K_i^* = 5.6 \times 10^5$ M^{-1} s^{-1}) than by native MPI ($k_{ass} = 3.1 \times 10^6$ M^{-1} s^{-1}). This view does, however, not hold, because at physiological concentrations, oxidized MPI forms an EI* complex whereas native MPI does not. Since the local concentration of oxidized MPI is 86-fold higher than K_i^*, the $E + I \rightleftharpoons EI^*$ equilibrium will be fully shifted toward EI* (*29*). Therefore, immediately after its release from neutrophils, the bulk of elastase will be taken up as an EI* complex whose pseudo-first-order rate constant of formation, k^*, will be given by $k^* = (k_1[I]_o + k_{-1})$, which may also be written as $k^* = [k_{-1}\ (1 + [I]_o/K_i^*)]$. Since accumulation of EI* requires $k_{-1} \gg k_2$, one gets $k^* \gg [k_2\ (1 + [I]_o/K_i^*]$ and hence $k^* \gg 2.8$ s^{-1}. If we set $k_{-1} = 10k_2$, we get $k^* = 30$ s^{-1} as the lower limit of the pseudo-first-order rate constant for the inhibition of elastase by oxidized MPI. On the other hand, native MPI inhibits elastase with a pseudo-first-order rate constant of $k = (k_{ass}\ [I]_o + k_{diss}) = 15.5$ s^{-1}. Oxidized MPI is, therefore, a faster elastase inhibitor than native MPI in upper airways secretions.

Effect of Heparin on the Inhibitory Potency of Oxidized MPI. Heparin binds MPI and so accelerates the inhibition of cathepsin G, chymotrypsin, and elastase (*33*−*35*). We have used flow calorimetry to demonstrate that oxidized MPI also forms a complex with heparin. The equilibrium power p generated by reacting 4.5 kDa heparin with oxidized MPI was measured as a function of heparin concentration. Figure 3 shows the binding data together with those obtained previously with native MPI (*38*). The data were fitted to eq 6:

$$p = p_{sat}\{([I]_o + n[Hep]_o + K_d) - [([I]_o + n[Hep]_o + K_d)^2 - 4[I]_o\, n[Hep]_o]^{1/2}\}/2[I]_o \quad (6)$$

where $[I]_o$ and $[Hep]_o$ are the total concentrations of oxidized MPI and heparin, respectively, n is the oxidized MPI:heparin binding stoichiometry, and p_{sat} is the equilibrium power at infinite heparin concentration. Nonlinear regression was first done assuming that K_d, p_{sat}, and n are independent variables. This initial analysis gave $K_d = 110 \pm 130$ nM, $p_{sat} = 660 \pm 32$ nW, and $n = 0.91 \pm 0.11$. To improve the fit, n was set equal 1 and used as a prompted constant. This gave $K_d = 200 \pm 77$ nM and $p_{sat} = 670 \pm 27$ nW. The large error on K_d is due in part to the use of a 10-fold ratio of [oxidized MPI] to K_d which results in a steep titration curve (Figure 3). With inhibitor concentrations of the same order of magnitude as K_d, heat production was too small to record reliable binding data. K_d and p_{sat} were used to calculate $\Delta G°$, the energy of reaction, and $\Delta H°$ the enthalpy change and hence to infer $\Delta S°$, the entropy change. $\Delta H°$ and $\Delta S°$ for the oxidized MPI−heparin complex were found to be -11.5 ± -1.7 kcal mol^{-1} and -8.1 ± -4.0 cal K^{-1} mol^{-1}, respectively. These values are close to those reported previously for the native MPI−heparin complex (*38*).

The binding of native MPI, a positively charged protein with 4.5 kDa heparin, a negatively charged polymer involves ionic interactions with five to six basic amino acid residues of the polypeptide comprising two lysines and two arginines located in a conformationally sensitive ionic cluster (*22*). Since oxidation of MPI has no significant effect on the heparin-inhibitor binding strength and energetics, it may be suggested that it does not lead to a gross conformational change of the inhibitor. Hence, the deleterious effect of oxidants on the inhibitory activity of MPI are likely to be due only to the transformation of P_1' Met into methionine sulfoxide (*25*) and not to a conformational change of the inhibitor as found with plasminogen activator inhibitor I which has also a Met residue at P_1' (*42*).

Heparin not only binds MPI but also elastase and cathepsin G, the K_d values for the two enzymes being in the nanomolar range (*34*, *35*). The influence of heparin on the kinetics of inhibition of proteinases by MPI was therefore tested using a 40 μM concentration of the polymer. With this concentration, enzyme and inhibitor are saturated to at least 99% as calculated with a program for computing distribution diagrams for multiple equilibria (*43*).

In the presence of heparin, the progress curves describing the inhibition of cathepsin G by oxidized MPI were biphasic, whereas they were linear in the absence of heparin (see above). The pseudo-first-order rate constants k derived from these curves were found to vary hyperbolically with the inhibitor concentration (Figure 4), indicating two-step inhibition (Scheme 2). The data could be fit to eq 3 by nonlinear regression analysis, which yielded the best estimates of K_i^*, k_2, and k_{-2} reported in Table 1. The calculated K_i (42 ± 20 nM) was in accord with that derived from steady-state velocities (24 ± 7 nM) (Table 1).

If one assumes that in inflammatory lung secretions the bulk of MPI (5 μM, refs *27* and *28)* is in an oxidized form and that heparin is present in these secretions, 96% of the cathepsin G released from neutrophils will be inhibited as an EI* complex (*29*) and ultimely 99.2% as an EI complex

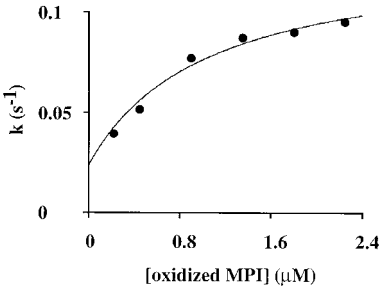

FIGURE 4: Effect of oxidized MPI on *k*, the pseudo-first-order rate constant of cathepsin G inhibition in the presence of 4.5 kDa heparin at pH 7.4 and 25 °C. The rate constants *k* were calculated from progress curves recorded following addition of cathepsin G + heparin to mixtures of oxidized MPI + heparin + Suc-Ala_2-Pro-Phe-SBzl. The final concentrations of cathepsin G, heparin, and substrate were 20 nM, 40 μM, and 0.21 mM, respectively.

(see also Figure 1). On the other hand, as already outlined above, the two-step inhibition mechanism implies that k^*, the rate constant of EI* formation, should be much higher than $[k_2(1 + [I]_o/K_i^*)]$, that is to say that $k^* \gg 2.4\ s^{-1}$. If we set $k_{-1} = 10k_2$, the lower limit of k^* will be $25\ s^{-1}$ ($t_{1/2} = 0.028$ s). Thus, heparin transforms oxidized MPI into a tight-binding and very fast-acting cathepsin G inhibitor. It is noteworthy that native MPI is a much slower inhibitor of cathepsin G than the oxidized MPI−heparin complex since its in vivo inhibition rate constant $k = (k_{ass}[I]_o + k_{diss})$ is equal to $0.5\ s^{-1}$ ($t_{1/2} = 1.4$ s). Since native MPI and the oxidized MPI−heparin complex have about the same K_i for cathepsin G, it may be concluded that heparin-bound oxidized MPI is a much better cathepsin G inhibitor than native MPI.

The progress curve analysis showed that heparin also has a favorable effect on the inhibition of chymotrypsin and elastase by oxidized MPI. With the former, enzyme progress curves were generated using ≥15 nM chymotrypsin, 40 μM heparin, and 0.25 mM Suc-Ala_2-Pro-Phe-pNA. The rate constants *k* varied linearly with the inhibitor concentration (not shown), indicating that under the experimental conditions employed the EI* complex is not seen kinetically so that the data could again be described by Scheme 1. The values of k_{ass} and k_{diss} are reported in Table 1 together with the calculated K_i (6.1 ± 2.9 nM). The latter could be confirmed experimentally (2.6 ± 0.8 nM) (Table 1).

With elastase, the progress curves were recorded as described in the legend to Figure 2 except that 40 μM heparin was present in the reaction mixtures. The rate constants *k* varied hyperbolically with the oxidized MPI concentration (figure not shown) indicating two-step inhibition (Scheme 2) as already observed in the absence of heparin. The values of K_i^*, k_2, and k_{-2} are reported in Table 1, together with the calculated value of K_i (1.4 ± 0.8 nM). Again, the latter could be checked experimentally ($K_i = 2.7 \pm 0.7$ nM, Table 1).

Table 1 shows that heparin increases the rate constant for the inhibition of chymotrypsin and elastase by oxidized MPI by a factor of about 30. The acceleration of elastase inhibition is mainly due to an enhancement of k_2, the rate constant for the isomerization of EI* into EI. A significant increase in the overall rate of elastase inhibition by oxidized MPI has also been observed with polydisperse commercial heparin preparations (*26*). As already noticed for cathepsin G, the second-order rate constants for the inhibition of chymotrypsin and elastase are higher with oxidized MPI in the presence of heparin than with native MPI in the absence of the polymer (Table 1). Thus, as far as the rate of inhibition is concerned, the oxidized MPI−heparin complex is a better cathepsin G, elastase, and chymotrypsin inhibitor than free native MPI.

Elastase, cathepsin G, and MPI bind heparin whereas chymotrypsin does not (*35*). We have previously shown that heparin increases the rate of chymotrypsin inhibition to about the same extent as it enhances the rate of elastase or cathepsin G inhibition (*34*, *35*), indicating that binding of heparin with both enzyme and inhibitor is not required for maximum rate enhancement as it is with antithrombin (*44*). Here, we come to the same conclusion using oxidized MPI.

CONCLUSION

The present data may help explain why lung tissue proteolysis occurs during chronic bronchitis despite the presence of large quantities of MPI in airways secretions. In this disease, there is an important recruitment of neutrophils at inflammatory sites. When these cells are activated or when they die, they release both proteolytic enzymes and oxidants. Neutrophil-mediated MPI oxidation has been demonstrated in vitro (*7*) and certainly also occurs in vivo. We have shown here that the oxidized inhibitor is a very weak inhibitor of neutrophil cathepsin G, which may therefore cleave lung matrix proteins in an almost unimpaired way.

Our findings also have some bearing on the therapy of the pulmonary form of cystic fibrosis. In this disease, there is such a high pulmonary load of leukoproteinases that the activity of MPI is overcome (*27*, *28*, *45*). Aerosol-delivered recombinant MPI has been shown to significantly depress the elastase activity of cystic fibrosis lung secretions (*45*). It is likely that the inhaled inhibitor undergoes fast oxidation due to the very large amounts of oxidants present in lung secretions. The fact that inhalation of MPI nevertheless led to a decrease in elastase activity is best explained by our finding that oxidized MPI is still a potent elastase inhibitor. Although the activity of cathepsin G was not measured in the above study (*45*), it is likely that aerosol-delivered MPI did not significantly depress it because the oxidized inhibitor poorly inhibits it. In contrast, the finding that heparin restores the anti-cathepsin G activity of oxidized MPI suggests that heparin might be a useful adjuvant of MPI-based therapy of cystic fibrosis.

ACKNOWLEDGMENT

We thank Synergen for the gift of recombinant MPI.

REFERENCES

1. Davies, K. J. A. (1987) *J. Biol. Chem. 262*, 9895−9901.
2. Reddy, V. Y., Desrochers, P. E., Pizzo, S. V., Gonias, S. L., Sahakian, J. A., Levine, R. L., and Weiss, S. J. (1994) *J. Biol. Chem. 269*, 4683−4691.
3. Swaim, M. W., and Pizzo, S. V. (1988) *J. Leukocyte Biol. 43*, 365−379.
4. Shechter, Y., Burstein, Y., and Gertler, A. (1977) *Biochemistry 16*, 992−997.
5. Strandberg, L., Lawrence, D., Johansson, L., and Ny, T. (1991) *J. Biol. Chem. 266*, 13852−13858.
6. Johnson, D., and Travis, J. (1979) *J. Biol. Chem. 254*, 4022−4026.
7. Carp, H., and Janoff, A. (1980) *Exp. Lung Res. 1*, 225−237.

8. Janoff, A. (1983) *Chest 83*, 54−58.
9. Cochrane, C. G., Spragg, R., and Revak, S. D. (1983) *J. Clin. Invest. 71*, 754−761.
10. Weiss, S. J. (1989) *New Eng. J. Med. 320*, 365−376.
11. Bieth, J. G. (1986) in *Regulation of Matrix Accumulation* (Mecham, R. P., Ed.) Vol. 1, pp 217−320, Academic Press, New York.
12. Wallner, O., and Fritz, H. (1974) *Hoppe Seyler's Z. Physiol. Chem. 355*, 709−715.
13. Ohlsson, K., Tegner, H., and Akesson, U. (1977) *Hoppe Seyler's Z. Physiol. Chem. 358*, 583−589.
14. Schiessler, H., Arnhold, M., Ohlsson, K., and Fritz, H. (1976) *Hoppe-Seyler's Z. Physiol. Chem. 357*, 1251−1260.
15. Ohlsson, M., Rosengren, M., and Olsson, K. (1983) *Hoppe-Seyler's Z. Physiol. Chem. 364*, 1323.
16. Böhm, B., Deutzmann, R., and Burkhardt, H. (1991) *Biochem. J. 274*, 269−273.
17. Kramps, J., Boekhorst, A., Fransen, J., Ginsel, L., and Dijkman, J. (1989) *Am. Rev. Respir. Dis. 140*, 471−476.
18. Seemüller, U., Arnhold, M., Fritz, H., Wiedenmann, K., Machleidt, W., Heinzel, R., Appelhans, H., Gassen, H., and Lottspeich, F. (1986) *FEBS Lett. 199*, 43−48.
19. Thompson, R., and Ohlsson, K. (1986) *Proc. Natl. Acad. Sci. U.S.A. 83*, 6692−6696.
20. Grütter, M., Fendrich, G., Huber, R., and Bode, W. (1988) *EMBO J. 7*, 345−351.
21. Steller, G., Brener, M. T., and Thompson, R. C. (1986) *Nucleic Acid Res. 14*, 7883−7896.
22. Mellet, P., Ermolieff, J., and Bieth, J. G. (1995) *Biochemistry 31*, 2645−2652.
23. Boudier, C., and Bieth, J. G. (1989) *Biochim. Biophys. Acta 997*, 285−288.
24. Eisenberg, S., Hale, K. K., Heimdal, P., and Thompson, R. C. (1990) *J. Biol. Chem. 265*, 7976−7981.
25. Boudier, C., and Bieth, J. G. (1994) *Biochem. J. 303*, 61−68.
26. Ying, Q. L., Kemme, M., Saunders, D., and Simon, S. R. (1997) *Lung Cell. Mol. Physiol. 16*, L533−L541.
27. Kramps, J., Van Twisk, C., Appelhans, H., Meckelein, B., Nikiforov, T., and Dijkman, J. (1990) *Biochim. Biophys. Acta 1038*, 178−185.
28. Tournier, J., Jacquot, J., Sadoul, P., and Bieth, J. G. (1983) *Anal. Biochem. 131*, 345−350.
29. Bieth, J. G. (1995) *Method Enzymol. 248*, 59−84.
30. Bieth, J. G. (1996) in *Alpha-1-Antitrypsin Deficiency* (Crystal, R. G., Hubbard, R. C., and Trapnell, B. C., Eds.) pp 119−128, Marcel Dekker, New York.
31. Hof, P., Mayr, I., Huber, R., Korzus, E., Potempa, J., Travis, J., Powers, J. C., and Bode, W. (1996) *EMBO J. 15*, 5481−5491.
32. Boudier, C., Holle, C., and Bieth, J. G. (1981) *J. Biol. Chem. 256*, 10256−10258.
33. Faller, B., Mely, Y., Gérard, D., and Bieth, J. G. (1992) *Biochemistry 31*, 8285−8292.
34. Cadène, M., Boudier, C., Daney de Marcillac, G., and Bieth, J. G. (1995) *J. Biol. Chem. 270*, 13204−13209.
35. Ermolieff, J., Duranton, J., Petitou, M., and Bieth, J. G. (1998) *Biochem. J. 330*, 1369−1374.
36. Casu, B. (1990) *Haemostasis 20* (Suppl. 1), 62−73.
37. Boudier, C., and Bieth, J. G. (1992) *J. Biol. Chem. 267*, 4370−4375.
38. Cadène, M., Morel-Desrosiers, N., Morel, J. P., and Bieth, J. G. (1995) *J. Am. Chem. Soc. 117*, 7882−7886.
39. Morrisson, J. F., and Walsh, C. T. (1988) *Adv. Enzymol. Relat. Areas Mol. Biol. 61*, 201−301.
40. Smith, C., and Johnson, D. (1985) *Biochem. J. 255*, 463−472.
41. Bieth, J. G. (1984) *Biochem. Med. 32*, 387−397.
42. Lawrence, D. A., and Loskutoff, D. J. (1986) *Biochemistry 25*, 6351−6355.
43. Stefano, C., Princi, P., Rigano, C., and Sammartano, S. (1988) *Ann. Chim. 78*, 55−82.
44. Danielsson, Á, Raub, E, Lindhahl, U., and Björk, I. (1986) *J. Biol. Chem. 261*, 15467−15463.
45. McElvaney, N. G., Nakamura, H., Birrer, P., Hebert, C. A., Wong, W. L., Alphonso, M., Baker, J. B., Catalano, M. A., and Crystal, R. G. (1992) *J. Clin. Invest. 90*, 1296−1301.

BI9828526